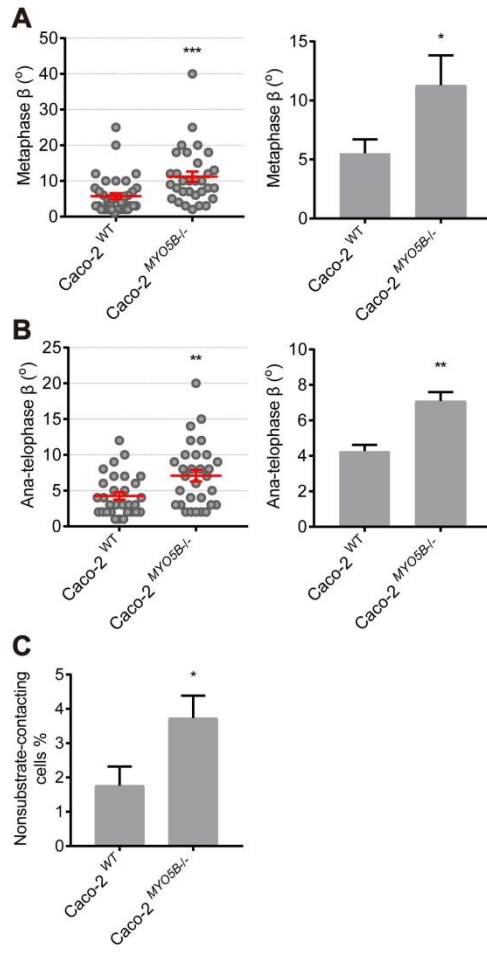


S1 Fig. Characterization of Caco-2^{MYO5B-/-} cells.

(A) Western blotting analysis showed a complete loss of the myosin Vb protein in Caco-2^{MYO5B-/-} cells. (B) The sequence of Caco-2^{MYO5B-/-} cells showed a deletion in exon 3 resulting in premature stop codon at amino acid position 66.

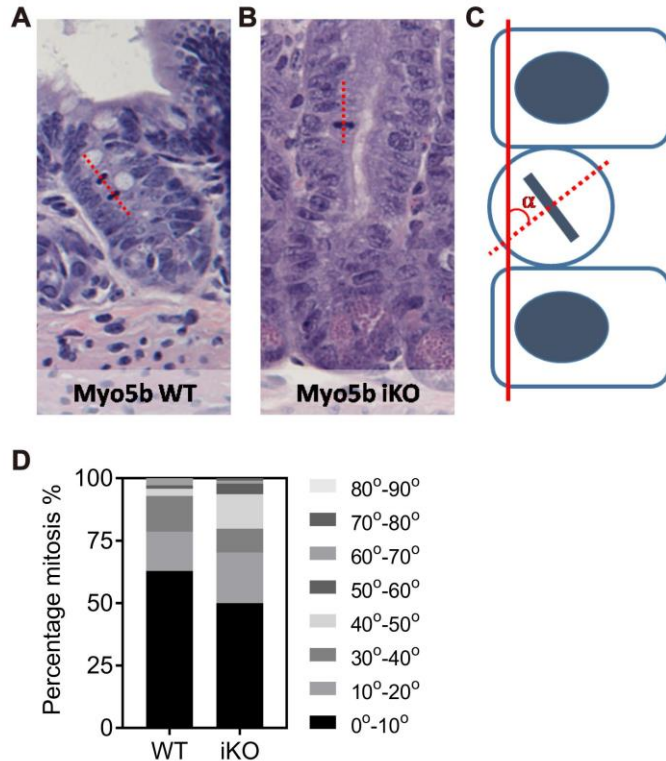
<https://doi.org/10.1371/journal.pbio.3000531.s001>



S2 Fig. Caco-2 $MYO5B^{-/-}$ cells show mitotic spindle orientation defects in transwell culture.

(A, B) The β -angle in metaphase (A) and anaphase (B) was quantified in Caco2^{WT} cells and Caco-2 $MYO5B^{-/-}$ cells after cultured in transwell for 5 days. The dot graph: each dot indicates one cell's β -angle. The histogram graph: the statistical analysis of the mean for each experiment. More than 10 cells/experiment were analyzed for $N = 3$ independent experiments. (C) The percentage of nonsubstrate-contacting cells was quantified in Caco2^{WT} and Caco2 $MYO5B^{-/-}$ cells after cultured in transwell for 5 days. $N = 3$ independent experiments. t test, * $p < 0.05$, ** $p < 0.01$, *** $p < 0.001$. Error bars indicate \pm SEM (dot graph) or + SD (bar graph). Scale bars: 5 μm . Values for each data point can be found in [S11 Data](#). WT, wild type.

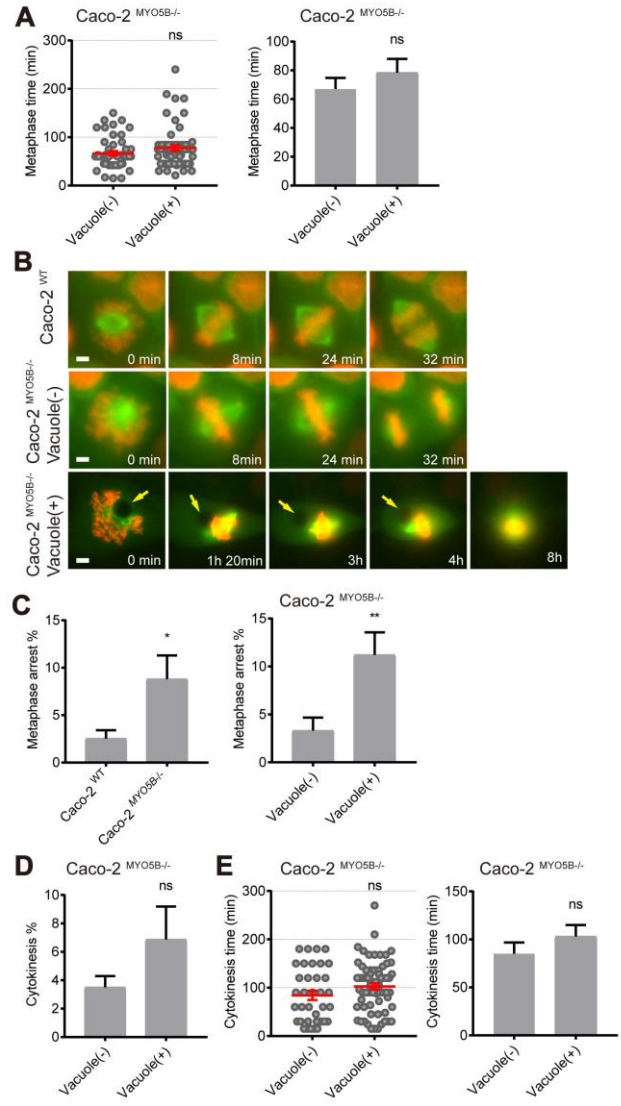
<https://doi.org/10.1371/journal.pbio.3000531.s002>



S3 Fig. Mitotic spindle orientation in small intestinal epithelial cells.

(A–C) The orientation of the mitotic spindle of small intestinal epithelial cells from Myo5b WT (A) and Myo5b iKO (B) mice by measuring the angle (α) formed by the mitotic cell in metaphase or anaphase (dotted red line) and the epithelial surface (solid red line) in hematoxylin and eosin stained sections (C). (D) The percentage of mitotic cells with angles in the indicated intervals is shown for Myo5b WT and iKO mice. At least 70 mitosis were scored in 4 animals per group. Fisher's exact test of $<10^\circ$ versus $\geq 10^\circ$, $p = 0.11$. Values for each data point can be found in [S12 Data](#). iKO, intestinal knockout; WT, wild type.

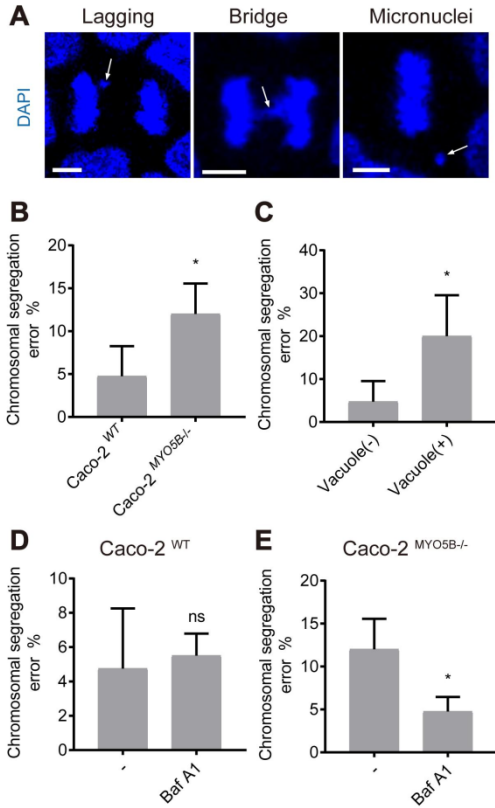
<https://doi.org/10.1371/journal.pbio.3000531.s003>



S4 Fig. Live cell imaging of mitotic Caco-2^{MYO5B-/-} cells.

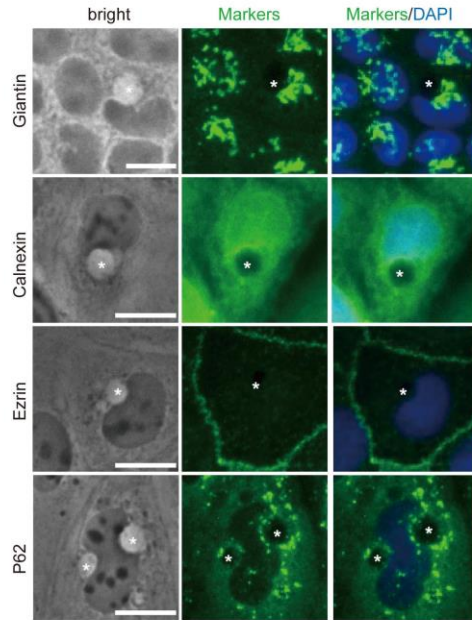
(A) The quantification of metaphase duration time in live Caco-2^{MYO5B-/-} cells with vacuole and without vacuole. Left side graph: each dot indicates one cell's metaphase duration time; right side graph: the statistical analysis of the mean for each experiment. $n > 10$ cells/experiment were analyzed for $N = 3$ independent experiments. (B) Live cell imaging shows x-y-t time-lapse mitosis images on Caco-2^{WT} and Caco-2^{MYO5B-/-} cells expressing β -tubulin-GFP and histone2B-mCherry. The metaphase arrest was identified by metaphase duration time > 5 h and no observed division at the end. (C) Left side graph: quantification of the percentage of metaphase arrest in live Caco-2^{WT} and Caco-2^{MYO5B-/-} cells. Right side graph: quantification of the percentage of metaphase arrests in live Caco-2^{MYO5B-/-} cells with and without vacuoles. (D) The percentage of cytokinesis was quantified in the fixed Caco-2^{MYO5B-/-} cells with or without vacuoles. (E) The time of cytokinesis duration was quantified in live Caco-2^{MYO5B-/-} cells with or without vacuoles. Left side graph: each dot indicates one cell's cytokinesis duration time; right side graph: the statistical analysis of the mean for each experiment. $n > 10$ cells/experiment were analyzed for $N = 3$ independent experiments. t test, $*p < 0.05$, $**p < 0.01$. Error bars indicate \pm SEM (dot graph) or \pm SD (bar graph). Scale bars: 2 μ m. Values for each data point in panels A, C, D, and E can be found in S13 Data. ns, not significant; WT, wild type.

<https://doi.org/10.1371/journal.pbio.3000531.s004>



S5 Fig. Loss of *MYO5B* causes chromosomal segregation errors.

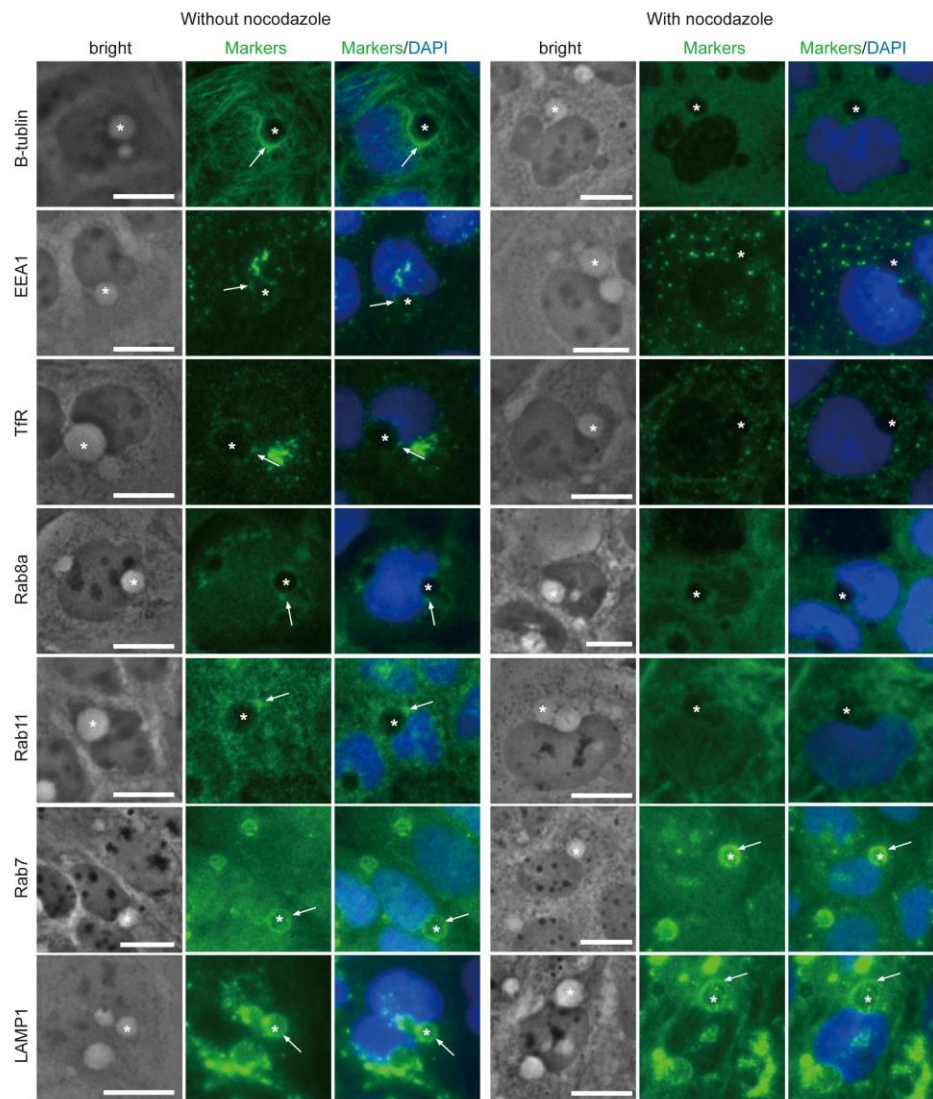
(A) The images show chromosomal segregation errors in Caco-2^{MYO5B-/-} cells, including chromosomal lagging and bridge in anaphase and micronuclei in metaphase (arrows). (B) The chromosomal segregation errors were quantified in Caco-2^{WT} and Caco-2^{MYO5B-/-} cells. (C) The chromosomal segregation errors were quantified in Caco-2^{MYO5B-/-} cells with and without vacuoles. (D and E) The chromosomal segregation errors in Caco-2^{WT} (D) and Caco-2^{MYO5B-/-} cells (E) were compared after treated with Baf A1 for 24 h. $N = 3$ independent experiments. t test, * $p < 0.05$. Error bars indicate + SD. Scale bars: 5 μ m. Values for each data point in panels B through E can be found in [S14 Data](#). Baf, baflomycin; ns, not significant; WT, wild type. <https://doi.org/10.1371/journal.pbio.3000531.s005>



S6 Fig. Immunolabeling of Caco-2^{MYO5B-/-} cells.

Vacuoles (asterisks) in Caco-2^{MYO5B-/-} were found to be negative for markers of organelles including Golgi (giantin), endoplasmic reticulum (calnexin), microvillus inclusion bodies (ezrin), autophagosomes (p62). Scale bars: 10 μm.

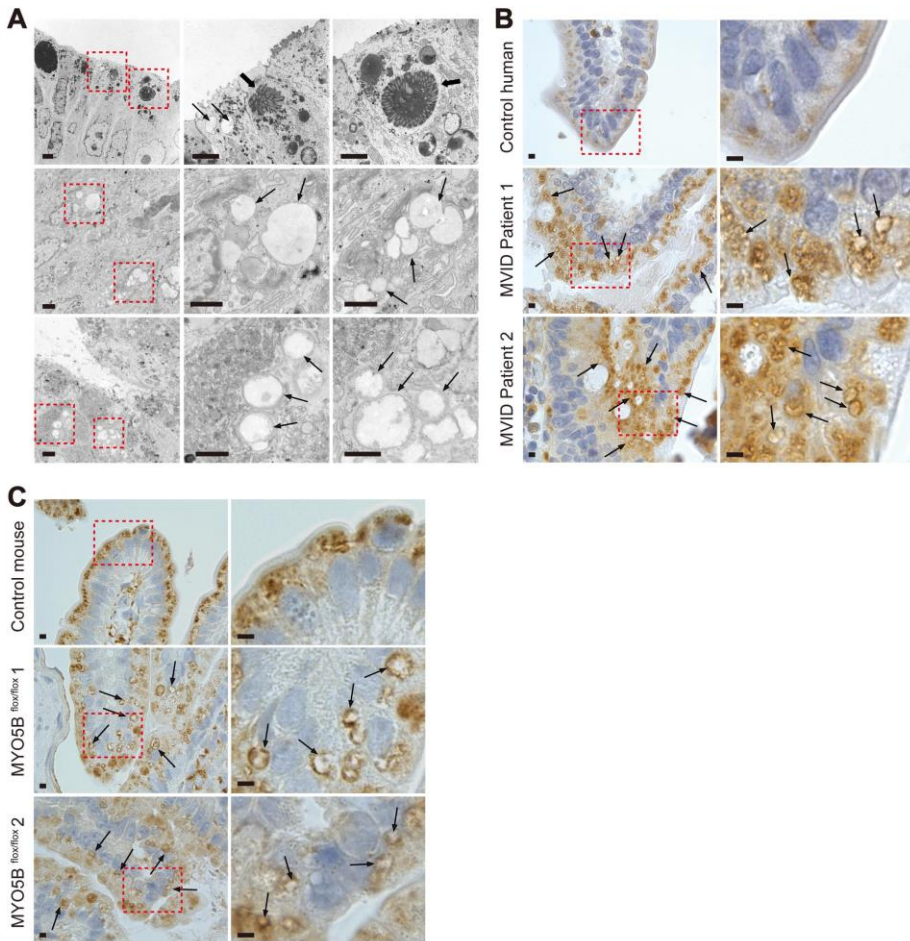
<https://doi.org/10.1371/journal.pbio.3000531.s006>



S7 Fig. Immunolabeling of Caco-2^{MYO5B-/-} cells.

Vacuoles (asterisks) in Caco-2^{MYO5B-/-} were surrounded by microtubules (β -tubulin) and stained negative for markers of early/recycling endosomes (EEA1, TfR, rab8a, and rab11) but positive for markers of late endosome/lysosomes (rab7 and LAMP1). Endosomal markers were often found very close to the vacuoles (arrows), which could be because of their association with the perivacuolar microtubule cytoskeleton. To distinguish whether these markers were truly associated with the vacuoles or located subjacent to the vacuoles, we treated the cells with nocodazole (33 μ M) for 2 h. In contrast to the resultant dispersal of early endosomal and recycling endosomal markers, rab7 and LAMP1 remained positive at the vacuoles. Scale bars: 10 μ m. EEA1, early endosomal antigen-1; LAMP1, late endosome-associated membrane protein; TfR, transferrin receptor.

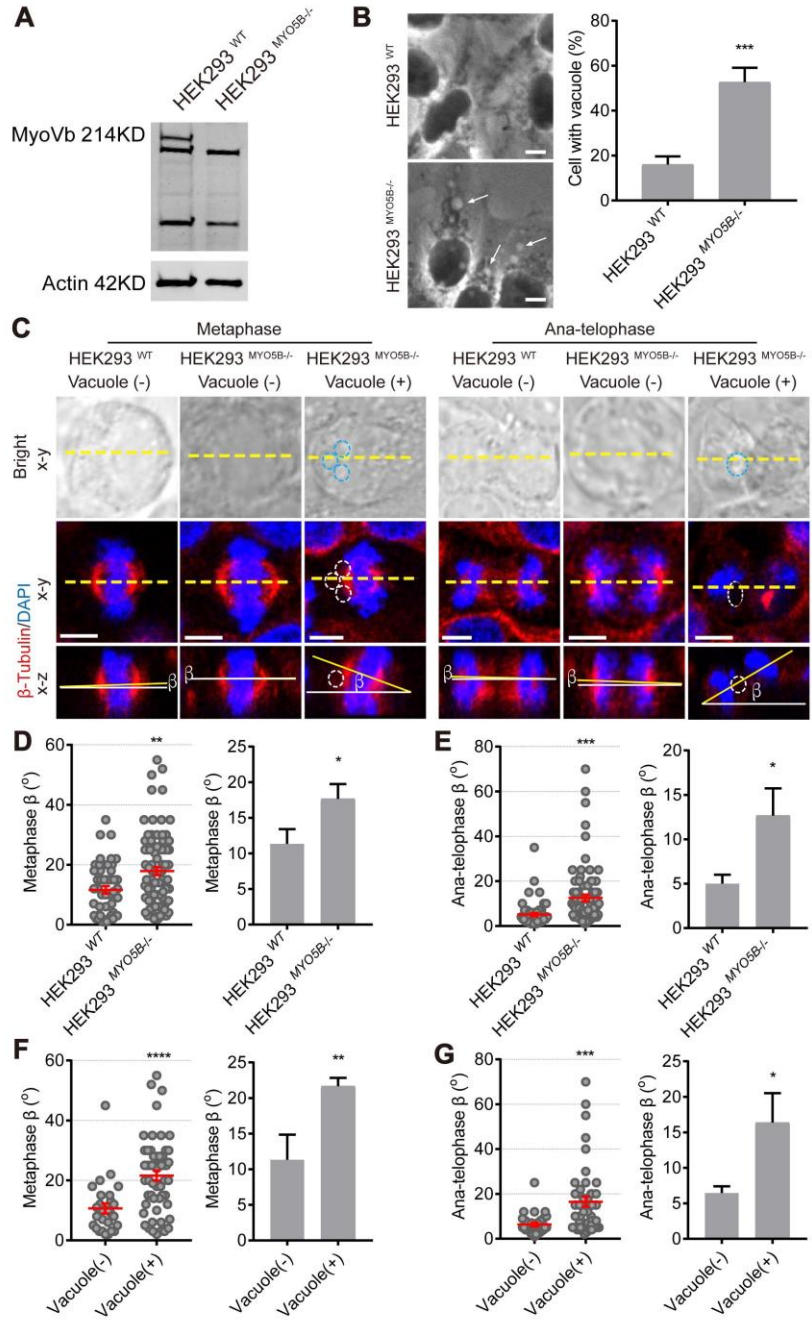
<https://doi.org/10.1371/journal.pbio.3000531.s007>



S8 Fig. Microscopical analyses of MVID tissue.

(A) Electron microscopy of MVID patients' duodenum. Black thick and thin arrows indicate microvillus inclusion bodies and electron-lucent vacuoles, respectively. (B–C) Immunohistochemistry of LAMP1 staining in MVID patients' (B) and *MYO5B* KO mouse (C) duodenum and appropriate controls. Arrows indicate large LAMP1-positive vacuoles. Nuclei is stained with hematoxylin. KO, knockout; LAMP1, late endosome–associated membrane protein; MVID, microvillus inclusion disease.

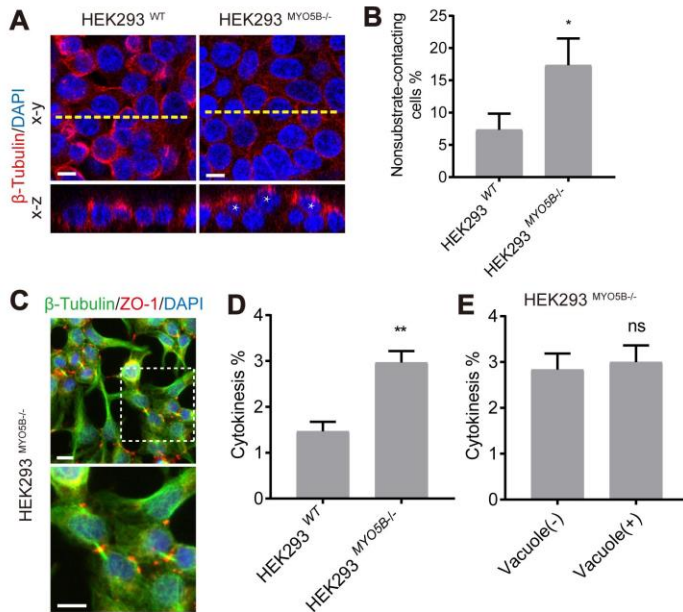
<https://doi.org/10.1371/journal.pbio.3000531.s008>



S9 Fig. Loss of *MYO5B* induces large vacuoles and causes mitotic spindle orientation defects in HEK293 cells.

(A) Western blotting analysis showed a complete loss of the myosin Vb protein in HEK293^{MYO5B^{-/-}} cells. (B) Arrows indicate large vacuoles in HEK293^{MYO5B^{-/-}} cells. The percentage of cells with vacuole (diameter $\phi > 1 \mu\text{m}$) was quantified in fixed HEK293^{WT} and HEK293^{MYO5B^{-/-}} cells. (C) The images showed HEK293^{WT} cells, HEK293^{MYO5B^{-/-}} cells without and with vacuoles stained as indicated in metaphase and anaphase. The dotted circles in the images indicate large vacuoles. (D and E) The β -angle in metaphase (D) and anaphase (E) was quantified in HEK293^{WT} and HEK293^{MYO5B^{-/-}} cells. The dot graph: each dot indicates one cell's β -angle. The histogram graph: the statistical analysis of the mean for each experiment. More than 10 cells/experiment were analyzed. (F and G) The β -angle in metaphase (F) and anaphase (G) was quantified in HEK293^{MYO5B^{-/-}} cells without and with vacuoles. $N = 3$ independent experiments. t test, * $p < 0.05$ ** $p < 0.01$, *** $p < 0.001$, **** $p < 0.0001$. Error bars indicate \pm SEM (dot graph) or \pm SD (bar graph). Scale bars: 5 μm . Values for each data point in panels B, D, E, F, and G can be found in [S15 Data](#). HEK, human embryonic kidney cell; WT, wild type.

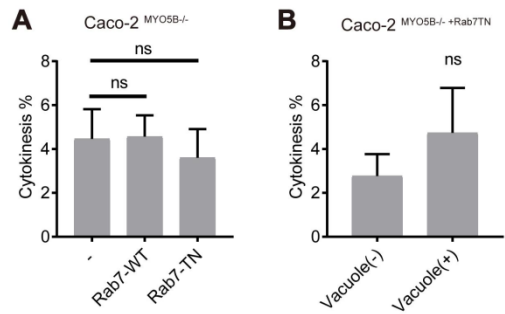
<https://doi.org/10.1371/journal.pbio.3000531.s009>



S10 Fig. Loss of MYO5B increases delamination and cytokinesis index in HEK293 cells.

(A) The presence of cells not contacting the substratum was indicated by asterisks in nuclei. (B) The percentage of nonsubstrate-contacting cells was quantified. (C) Images showed the cytokinesis cells in HEK293^{MYO5B^{-/-}} cells. (D) The percentage of cytokinesis cells was quantified in HEK293^{WT} and HEK293^{MYO5B^{-/-}} cells. (E) The percentage of cytokinesis cells was quantified in HEK293^{MYO5B^{-/-}} cells without and with vacuoles. $n > 1,000$ cells/experiment were analyzed for $N = 3$ independent experiments. t test, $*p < 0.05$, $**p < 0.01$. Error bars indicate \pm SD. Scale bars: 5 μ m. Values for each data point in panels B, D, and E can be found in [S16 Data](#). HEK, human embryonic kidney cell; ns, not significant; WT, wild type.

<https://doi.org/10.1371/journal.pbio.3000531.s010>



S11 Fig. Effect of rab7 and rab7 mutant on cytokinesis.

(A) The percentage of cytokinesis was quantified in the fixed Caco-2 $MYO5B^{-/-}$ cells expressing GFP-rab7-WT or GFP-rab7-T22N. (B) The percentage of cytokinesis was quantified in the fixed Caco-2 $MYO5B^{-/-}$ cells expressing GFP-rab7-T22N with and without vacuoles. $N = 3$ independent experiments. t test, error bars indicate \pm SD. Values for each data point can be found in [S17 Data](#). GFP, green fluorescent protein; ns, not significant; WT, wild type.

<https://doi.org/10.1371/journal.pbio.3000531.s011>